

# Investigation of spin correlations in concentrated Fe-Ni-Cr spin glasses by the method of polarized neutron scattering

V. V. Runov, S. L. Ginzburg, B. P. Toperverg, A. D. Tret'yakov, A. I. Okorokov, and E. I. Mal'tsev

*B. P. Konstantinov Leningrad Institute of Nuclear Physics, Academy of Sciences of the USSR, Gatchina*  
(Submitted 25 June 1987)

Zh. Eksp. Teor. Fiz. **94**, 325–345 (January 1988)

A study was made of the spatial structure of spin correlations in magnetic materials with competing random spin-spin interactions. The intensity of low-angle scattering of polarized neutrons and their depolarization in disordered Fe-Ni-Cr alloys was measured. An analysis was made of the temperature and momentum behavior of spin correlations in a system exhibiting a sequence of paramagnetic-ferromagnetic-spin glass (P-F-SG) phase transitions. The low-temperature phases of such magnetic materials exhibited not only thermodynamic but also frozen spin configuration correlations. The temperatures of the phase transitions and the critical exponent  $\nu$  of the correlation radius were determined. The neutron depolarization was found to be highly sensitive to magnetic P-F-SG and P-SG phase transitions and to irreversible effects in the SG state during magnetic annealing. The problems of interpretation of the low-angle scattering data were discussed in detail.

## 1. INTRODUCTION

In recent years there has been considerable interest not only in dilute ("classical") spin glasses of the  $Mn_xCu_{1-x}$  type, but also in concentrated spin systems with a competing random interaction, such as  $Eu_xSr_{1-x}S$ ,  $(Fe_xMn_{1-x})_{75}P_{16}B_6Al_3$ ,  $Fe_xCr_{1-x}$ , etc.<sup>1-4</sup> Systems of this kind, both crystalline and amorphous, exhibit a strong competition of random ferromagnetic and antiferromagnetic interactions between various pairs of atomic spins and, in contrast to dilute magnetic materials, where interactions with opposite signs are practically equiprobable, the ratio of the probabilities of opposite signs in concentrated alloys is determined by the composition of the alloy. Therefore, depending on the concentration  $x$ , a transition to the spin glass (SG) state may occur either directly from the paramagnetic (P) phase or via a state characterized by a macroscopic magnetic moment. The state formed as a result of cooling from the ferromagnetic (F) phase is usually called in the literature the reentrant SG phase.

It therefore follows that the systems referred to above have a phase diagram which includes not only the P and SG phases, but also the F phase. The existence of a three-phase diagram in the case of systems with a competing interaction was recently predicted by Sherrington and Kirkpatrick.<sup>5</sup>

The majority of magnetic measurements have demonstrated that both the magnetization and the susceptibility of such systems depend similarly on temperature. In particular, in addition to an increase in the susceptibility and the appearance of the magnetization on transition to the F phase, these quantities exhibit a fall with temperature in the region of the transition to the reentrant spin glass phase. If the transition takes place from the P to the SG state, the temperature dependence of the magnetic susceptibility exhibits a characteristic kink, etc. It is also shown in Ref. 3 that in the vicinity of phase boundaries a system of alloys based on metallic glasses exhibits universal critical behavior of the magnetic susceptibility. A scaling analysis is used in Ref. 3 to construct phase diagrams representing four systems of

amorphous alloys. The critical exponents, different for each of the above-mentioned phase transitions, are practically the same for every one of these alloy systems.

Qualitatively similar phenomena are observed in the system under discussion and in the temperature dependences of the cross section for low-angle neutron scattering.<sup>1,2,4</sup> For example, if the phase transition sequence P-F-SG takes place, then in addition to the anomalies of the usual critical scattering in the vicinity of  $T_c$ , the low-angle scattering cross section increases also as a result of a transition to the reentrant spin glass state. If the transition to the spin glass phase occurs directly from the paramagnetic phase, then the temperature dependence of the low-angle scattering cross section has a fairly wide maximum in the region of a kink in the temperature dependence of the susceptibility.

The universal critical behavior of the magnetic susceptibility discovered by Yeshurun *et al.*<sup>3</sup> suggests that the scaling laws should apply in the vicinity of phase boundaries in such systems and also to spatial spin correlations. However, one should bear in mind that, in contrast to ordered systems, these correlations include also contributions not only of ordinary thermodynamic fluctuations, but also of configuration fluctuations. Their appearance is due to the existence of frozen local moments with random magnitudes and directions. This circumstance, which is not very important in investigations of the susceptibility, is very significant in the description of the neutron data. The point is that the neutron-scattering cross section is proportional, as is known, to the Fourier transform of a spin correlation function and, therefore, it includes contributions of both types of correlation. On the other hand, the magnetic susceptibility is related directly solely to thermodynamic spin fluctuations.

In magnetics with random competing interactions the freezing of local moments and, consequently, the appearance of spin configuration fluctuations of the magnetization occurs on transition to the F and SS states. However, it is very important to note that in the SS phase these fluctuations are not absolutely frozen and should relax slowly. In fact, it

is assumed at present that the most important property of the SS phase is its fundamental nonequilibrium (and nonergodicity), which accounts for the following experimentally observed irreversible effects: magnetic viscosity, magnetic memory, etc. (see, for example, the reviews in Refs. 6 and 7). According to the current ideas,<sup>8-10</sup> these slow spin relaxation effects are due to the existence in the SS state of a macroscopically large number of degenerate low-energy states (valleys). The distribution of valleys and barriers between them is assumed to be such that it gives rise to a wide spectrum of relaxation times, which is estimated in Ref. 11 to extend from  $10^{-12}$  to  $10^{20}$  s. Clearly, the existence of such a spectrum should give rise to a logarithmically slow evolution not only of homogeneous quantities (magnetization, susceptibility, etc.), but also of inhomogeneous spin correlations.

It should be pointed out that the appearance of effects of slow relaxation is expected not only on transition from the P to the SS phase, but also in the low-temperature range of the F phase.<sup>12</sup> In other words, the phase diagram of a magnetic material with random competing interactions should have<sup>12</sup> a region of coexistence of F and SS properties. This region should be regarded as a separate phase. Sometimes it is called the mixed phase. In the case of Heisenberg magnetic materials this phase exhibits asperomagnetic ordering of the atomic spins when not only configuration fluctuations of the components of atomic spins parallel to the magnetization may be observed, but also configuration fluctuations of the transverse components. The asperomagnetic (A) phase is, like the SS state, nonergodic. Therefore, these two types of configuration fluctuations are of nonequilibrium nature in the A phase and they should relax slowly.

The transition to the SS state from the A phase is possible either as a result of cooling or due to an increase in the degree of competition between random spin-spin interactions. Such a transition should be accompanied by disappearance of the magnetization, but this does not mean that complete isotropization of spin correlations takes place. The SS phase adjoining the A state may, in principle, be anisotropic and the phase transition from it to the isotropic SS state can occur as a result of further cooling.

Phase diagrams under discussion and the properties of spin correlations in each of the phases are largely hypothetical. The proposed scheme is based, on the one hand, on the results of theoretical investigations carried out so far only for the simplest models very far from reality. On the other hand, some of the proposed hypotheses are generalizations of the results of numerous experiments involving investigations of the phase diagram of disordered magnetic materials (see, for example, the reviews in Refs. 6 and 7).

The present paper reports an investigation of spin correlations in magnetic materials with competing spin-spin interactions carried out by the method of low-angle scattering of polarized neutrons and a check of the validity of the above picture of these correlations in description of the experimental data. In the second section we shall discuss in greater detail the temperature and momentum behavior of spin correlation functions in different phases of disordered Heisenberg magnetic materials. We shall summarize the results obtained in the molecular field approximation<sup>13</sup> and use the scaling theory ideas to obtain expressions for spin correlation functions, which will then be employed in an analysis of the experimental data.

In the third section we shall give the results of measurements of the scattering cross section and polarization of neutrons carried out on disordered  $\text{Fe}_{80-x}\text{Ni}_x\text{Cr}_{20}$  alloys in a wide range of temperatures and for different concentrations  $x$ . We shall show that the neutron data support the conclusions of earlier magnetic measurements<sup>14</sup> that this alloy system exhibits not only the P and F states (for  $x \geq 25$ ), but also the SG state. The temperature dependences of the low-angle scattering cross section are typical of systems with a three-phase diagram.<sup>4</sup> The polarization measurements reveal a high degree of sensitivity of the polarization not only to phase transitions which occur in the investigated system, but also to irreversible effects characterizing the SG state.

The fourth section is devoted to an analysis and interpretation of the experimental data. In particular, we shall show in this section that the intensity of the low-angle neutron scattering can be described quite satisfactorily by an expression which is a sum of the Ornstein-Zernike formula and of its square, and we shall demonstrate that the reciprocal of the radius of spin correlations deduced from an analysis of the data by means of this expression tends to zero both in the region of the transition from the P to the F state, and also in the vicinity of the transition from the F to the SS phase. The preliminary results of our study had been published as a preprint.<sup>13</sup>

## 2. SPIN CORRELATIONS AND NEUTRON SCATTERING IN DISORDERED MAGNETIC MATERIALS

Before we discuss the structure of spin correlations in various phases of disordered magnetic materials, we shall recall the familiar relationships between a correlation function  $\mathcal{H}_{ij}^{\alpha\beta}(t, t')$  of the projections of the atomic spins  $S_i^\alpha$  located at points with the coordinates  $r^i$  and  $r_j$ , on the one hand, and the intensity of the scattering of unpolarized neutrons  $I_{\mathbf{q}, \omega}$ , on the other:

$$I_{\mathbf{q}, \omega} \propto (\delta^{\alpha\beta} - e^\alpha e^\beta) \sum_{ij} \exp[i\mathbf{q}(\mathbf{r}_i - \mathbf{r}_j)] \int dt \exp(-i\omega t) \mathcal{H}_{ij}^{\alpha\beta}(t, t'), \quad (1)$$

$$\mathcal{H}_{ij}^{\alpha\beta}(t, t') = \langle S_i^\alpha(t') S_j^\beta(t' + t) \rangle. \quad (2)$$

In the above formulas  $\mathbf{q} = \mathbf{k}' - \mathbf{k}$  represents the momentum transferred in the scattering process,  $\omega = E' - E$  is the transferred energy,  $\mathbf{k}$  and  $\mathbf{k}'$  are the momenta,  $E$  and  $E'$  are the neutron energies before and after the scattering; the averaging is carried out over thermal spin fluctuations and over all possible realizations of spin-spin interactions.

Equations (1) and (2) are strictly speaking valid only if the scattering system is in a state of thermodynamic equilibrium. Then, the correlation function  $\mathcal{H}_{ij}^{\alpha\beta}$  is independent of  $t'$  and it can be represented conveniently as follows:

$$\mathcal{H}_{ij}^{\alpha\beta} = M^\alpha M^\beta + \mathcal{G}_{ij}^{\alpha\beta} + G_{ij}^{\alpha\beta}(t), \quad (3)$$

$$M^\alpha = \langle m_i^\alpha \rangle_c, \quad m_i^\alpha = \langle S_i^\alpha \rangle_T, \quad (4)$$

$$\mathcal{G}_{ij}^{\alpha\beta} = \langle (m_i^\alpha - M^\alpha)(m_j^\beta - M^\beta) \rangle_c, \quad (5)$$

$$G_{ij}^{\alpha\beta} = \langle (S_i^\alpha(0) - m_i^\alpha)(S_j^\beta(t) - m_j^\beta) \rangle_{T, c}, \quad (6)$$

where the indices  $T$  and  $c$  represent thermodynamic and configurational averaging, respectively;  $\mathbf{M}$  is the magnetization averaged over a sample;  $m_i$  is the local magnetization;

the functions  $\tilde{G}_{ij}^{\alpha\beta}$  and  $G_{ij}^{\alpha\beta}(t)$  represent configuration and thermodynamic correlations of spin fluctuations.

Substituting Eqs. (3)–(6) into Eq. (1), we obtain

$$I_{\mathbf{q},\omega} \propto (\delta^{\alpha\beta} - e^\alpha e^\beta) \{ [M^\alpha M^\beta S_0(\mathbf{q}) + \tilde{G}_q^{\alpha\beta}] 2\pi \delta(\omega) + G_q^{\alpha\beta}(\omega) \}, \quad (7)$$

where  $S_0(\mathbf{q})$  is the atomic structure factor. The momentum dependence associated with the magnetic atomic form factor will be ignored, since we shall be interested only in the scattering through small angles.

It follows from the definition of Eq. (5) that the configuration fluctuations appear only in disordered magnetic materials and they are observed simultaneously with freezing of the local moments  $\mathbf{m}_i$ , i.e., below the Curie point. In the P phase we find naturally that only the last term of Eq. (7) differs from zero.

As pointed out in the Introduction, the SG phase is fundamentally nonequilibrium. Therefore, the correlation function of Eq. (2) generally depends on two times  $t$  and  $t'$ , and the scattering intensity of Eq. (1) depends on the observation time  $t'$ . In experiments, averaging during the observation time occurs in an interval determined by the required statistical precision of the results of measurements. A detailed analysis demonstrates that, because of the logarithmic nature of the slow relaxation processes in the SG phase, the change in the scattering intensity during our measurements does not exceed a few percent. Within these limits we can assume that the correlation function of Eq. (2) does not vary with the time  $t'$ , i.e., we can assume that the scattering process is steady-state.

In the SG phase the equilibrium values  $\mathbf{m}_i$  and  $\mathbf{M}$  vanish. However, even then we can introduce an analog of a configuration correlation function  $\tilde{G}_{ij}(\omega)$ . However, now the correlation function does not describe correlations of frozen local moments  $m_i$ , but those spin fluctuations which have a wide spectrum of relaxation times. Naturally, the contribution of such fluctuations to  $I_{\mathbf{q},\omega}$  is not proportional to the  $\delta$  function of  $\omega$ , as in Eq. (7), but becomes infinite in the limit  $\omega \rightarrow 0$  [varying, for example, as  $(\omega \ln^2 \omega)^{-1}$ —see Ref. 15]. On the other hand, the contribution of thermodynamic correlations to  $I_{\mathbf{q},\omega}$  is considerably less singular in the limit  $\omega \rightarrow 0$  and, according to Ref. 16, in the SG range it is proportional to  $\omega^{-1/2}$ .

We shall not discuss in detail the problems of spin dynamics, because our experimental data on low-angle neutron scattering were obtained without measurement of the transferred energy  $\omega$ . We shall simply note that the intensity  $I(\vartheta)$  of neutron scattering to a given angle  $\vartheta$  is proportional to an equal-time spin correlation function  $\mathcal{K}_q$  if we can ignore the dependence of the transferred momentum  $\mathbf{q}$  on  $\omega$ . Since for  $\vartheta \ll 1$  and  $\omega \ll E$ , we have  $q^2(\omega) \approx k^2 [\vartheta^2 + (\omega/2E)^2]$ , we can ignore the dependence of  $\mathbf{q}$  on  $\omega$  if the main contribution to the integral of  $I_{\mathbf{q},\omega}$  with respect to  $\omega$  comes from the transferred energy range which satisfies the inequality  $\omega \ll 2E\vartheta$ . This means that if  $\Omega_q$  is the characteristic energy of spin fluctuations, then the inequalities  $\omega \lesssim \Omega_q \ll 2E\vartheta$  should be satisfied throughout the relevant integration domain.

Inelastic neutron scattering experiments<sup>2,17</sup> carried out on systems similar to that which we investigated have shown that the energies transferred as a result of the scattering are indeed small throughout the investigated ranges of tempera-

tures and scattering angles. Estimates, obtained on the basis of our polarization measurements, have indicated that the scattering inelasticity is weak also under our experimental conditions (a method which makes it possible to obtain such estimates is described in Refs. 18 and 19).

We shall therefore assume that the measured low-angle scattering intensity is given by the expression

$$I_{\mathbf{q}} \propto (\delta^{\alpha\beta} - e^\alpha e^\beta) \{ M^\alpha M^\beta S_0(\mathbf{q}) + \tilde{G}_q^{\alpha\beta} + G_q^{\alpha\beta} \}, \quad (8)$$

where  $q \approx k\vartheta$ , and  $\tilde{G}_q^{\alpha\beta}$  and  $G_q^{\alpha\beta}$  are simultaneous correlation functions of configuration and thermodynamic fluctuations, respectively.

We shall now discuss the momentum dependences of these correlation functions for different phases.

### a) Spin correlations in the paramagnetic phase

We have pointed out above that in the paramagnetic range only the correlation function of thermodynamic fluctuations  $G_q^{\alpha\beta} = \delta^{\alpha\beta} G_q$ , differs from zero. It is known that in the case of ordered magnetic materials this correlation function is described well by the Ornstein-Zernike formula:

$$G_q = A (q^2 + \kappa^2)^{-1}, \quad \kappa \approx a^{-1} \tau^\nu, \quad \tau = (T - T_c) T_c^{-1}, \quad (9)$$

where  $A$  is a constant of the order of the square of the reciprocal of the interatomic distance  $a$ ;  $\kappa$  is the reciprocal radius of the correlations;  $\nu$  is the correlation-radius exponent. In the case of three-dimensional Heisenberg ferromagnets we have  $\nu \approx 2/3$ .

Cooling enhances the spin correlations and at  $T = T_c$  for  $q = 0$  the correlation function of Eq. (9) becomes infinite. Naturally, a phase transition should occur in a similar manner in disordered magnetic materials. However, in view of the competition between the spin-spin interactions there is a major difference from the behavior of ordered magnetic materials: even the P phase of a disordered material exhibits SG fluctuations in addition to fluctuations of the ferromagnetic order parameter, i.e., of the magnetization. The correlation function of such fluctuations is (for details see Ref. 13)

$$g_{ij}^{\alpha\beta\gamma\delta} = \langle \langle S_i^\alpha S_j^\beta \rangle_T \langle S_i^\gamma S_j^\delta \rangle_T + \langle S_i^\alpha S_j^\delta \rangle_T \langle S_i^\beta S_j^\gamma \rangle_T \rangle_c \\ = 1/2 g_{ij} \{ \delta^{\alpha\beta} \delta^{\gamma\delta} + \delta^{\alpha\delta} \delta^{\beta\gamma} \}. \quad (10)$$

Moreover, there are also quadrupole fluctuations with the following correlation function (see Ref. 13)

$$\tilde{g}_{ij}^{\alpha\beta\gamma\delta} = \langle \langle S_i^\alpha S_i^\beta S_j^\gamma S_j^\delta \rangle_T - \langle S_i^\alpha S_j^\beta \rangle_T \langle S_i^\gamma S_j^\delta \rangle_T \rangle_c. \quad (11)$$

The correlations of these two types are not usually measured directly in experiments. Nevertheless, they have a considerable influence on the evolution of the experimentally determined ferromagnetic correlations. This is because these correlations, like those of the magnetization fluctuations, grow as a result of cooling at a rate which may be faster than the growth of ferromagnetic correlations and the transition occurs not to the F but to the SG phase.

The molecular field approximation was used in Ref. 13 to calculate all three types of correlation functions  $G_q^{\alpha\beta}$ ,  $g_q^{\alpha\beta\gamma\delta}$ , and  $\tilde{g}_q^{\alpha\beta\gamma\delta}$  for the Sherrington-Kirkpatrick model.<sup>5</sup> As expected, the correlations of each of the order parameters are described in this approximation by the Ornstein-Zernike formulas. However, whereas in the case of the ferromagnetic

correlations we find, as in Eq. (9), that  $\kappa \propto \tau^\nu$ , the reciprocal of the correlation radius of the spin glass fluctuations obeys  $\kappa_x \propto (\tau + \xi)^\nu$ , where as usual the following expressions are obtained in the mean-field approximation:

$$\nu = \nu' = 1/2, \quad \tau = (T - T_c) T_c^{-1}, \quad \xi = (T_c^2 - T_f^2) T_c^{-2},$$

where  $T_c$  is the Curie temperature and  $T_f$  is the temperature of the transition to the SG state. If we consider formally the dependences of  $\kappa$  and  $\kappa_x$  on  $T$ ,  $T_c$ , and  $T_f$ , we can say that P-F transition line is described by the equation  $\kappa = 0$ , whereas the phase boundary between the P and SG states is described by  $\kappa_x = 0$ . However, it is clear that if  $\xi > 0$ , then we have  $\kappa_x > \kappa$  for the whole P phase and if  $q = 0$  and  $\kappa = 0$ , the correlation function  $G$  vanishes and we have  $g \neq \infty$ . If  $\xi < 0$ , then throughout the P region we find that  $\kappa_x < \kappa$  and if  $q = 0$  and  $\kappa_x = 0$ , the spin glass correlation function  $g$  diverges and we have  $G \neq \infty$ . According to Ref. 13, throughout the temperature range where  $T > T_c$  and  $T > T_f$ , the function  $\tilde{g}$  does not become infinite at  $q = 0$  and the anisotropic spin glass phase is not obtained.

In the case of real disordered magnetic materials the transition temperatures  $T_c(x)$  and  $T_f(x)$  depend on the atomic concentrations of the components of the magnetic system. The dependences  $T_c(x)$  and  $T_f(x)$  plotted using the coordinates  $(T, x)$  determine the positions of the phase boundaries between the P and F or SG states (see, for example, Fig. 1). The intersection of these lines  $T_c(x)$  and  $T_f(x)$  governs the position of the triple point in the phase diagram.

The above specific formulas for the dependences of  $\kappa$  and  $\kappa_x$  on  $\tau$  and  $\xi$ , and also the Ornstein-Zernike formula of Eq. (9), are valid only as long as the correlations of fluctuations of the order parameter are small, i.e., they are valid away from the  $T_c(x)$  and  $T_f(x)$  transition lines. On approach to these lines we must allow for the mutual interaction of fluctuations growing in the vicinity of  $T_c$  and  $T_f$ . This should give rise to more complex dependences of  $\kappa$  and  $\kappa_x$  on  $T$  and  $x$ , and also to changes in the nature of the functions  $G_q$  and  $g_q$ . We shall not consider this topic and simply point out that far from the triple point, but close to the  $T_c(x)$  line, we have to allow only for the interaction of the F fluctuations with one another. This alters greatly the exponent in the

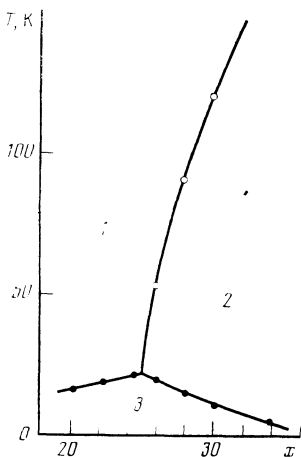


FIG. 1. Magnetic phase diagram of  $\text{Fe}_{80-x}\text{Ni}_x\text{Cr}_{20}$  alloys based on the data of Ref. 14: 1) paramagnetic (P) phase; 2) ferromagnetic (F) phase; 3) spin glass (SG) phase.

temperature dependence of the correlation radius [see Eq. (9)]. However, in a wide range of the parameters  $q$  and  $\kappa$  the function  $G_q(\kappa)$  changes only slightly. In particular, in the limit when  $q \gg \kappa$ , instead of Eq. (9) we should strictly speaking use the following expansion  $G_q(\kappa)$  in terms of the parameter  $\kappa/q \ll 1$  (Ref. 13):

$$G_q(\tau) = A(qa)^{-(2-\eta)} [1 + \lambda\tau(qa)^{-1/\nu} - (\kappa/q)^2 + \dots]. \quad (12)$$

However, in the above formula the small quantities include not only the Fisher parameter  $\eta \ll 1$ , but also the constant  $\lambda \ll 1$ , and for not too small ratios  $\kappa/q$  Eq. (12) is practically identical with the corresponding expansion of Eq. (9).

### b) Correlations in the ferromagnetic phase

In the F range, i.e., at temperatures  $T < T_c(x)$ , the appearance of a spontaneous moment  $\mathbf{M}$  is accompanied by an anisotropy of the tensor of spin correlations and in addition to the thermodynamic fluctuations of the magnetization in disordered magnetic materials, we can have also frozen configuration correlations.

We shall first consider the properties of the thermodynamic correlations. We shall write the correlation function  $G_q^{\alpha\beta}$  in the form

$$G_q^{\alpha\beta} = G_q^\perp (\delta^{\alpha\beta} - m^\alpha m^\beta) + G_q^\parallel m^\alpha m^\beta, \quad \mathbf{m} = \mathbf{M}M^{-1}. \quad (13)$$

It is shown in Ref. 13 that in the molecular field approximation if  $\tau \ll \xi$ , the functions  $G_q^\perp$  and  $G_q^\parallel$  are described by

$$G_q^\parallel = A^\parallel (q^2 + \kappa^2)^{-1}, \quad G_q^\perp = A^\perp q^{-2}, \quad A^\parallel \approx A^\perp \approx A, \quad \kappa^2 \sim a^{-2} \xi \tau. \quad (14)$$

In this approximation the difference between the nature of  $G_q^\parallel$  and  $G_q^\perp$  from that appropriate to the ordered case is the appearance of a factor  $\xi^{-1/2}$  in the expression for the correlation radius  $\kappa^{-1}$ . This means that the scale of critical fluctuations in disordered magnetic materials depends not only on temperature, but also on the degree of disorder, i.e., in fact it depends on the proximity to the triple point in the phase diagram. As in the case of the P region, an allowance for the interaction of the fluctuations alters the temperature and momentum dependences of the correlation functions in Eq. (14). We shall assume that  $\kappa \propto |\tau|^\nu$ , where  $\nu$  is the exponent of the correlation radius which has to be determined experimentally.

It is natural to assume that far from the triple point the changes in the momentum dependence of the correlation functions in Eq. (14) should be slight for  $q \gg \kappa$ , exactly as in the case of ordered magnetic materials. However, an allowance for the interaction of the fluctuations in the hydrodynamic range  $q \ll \kappa$  deserves a separate discussion. This is due to the fact that the interaction of transverse fluctuations with one another in ordered magnetic materials makes an additional contribution to the longitudinal correlation function  $G_q^\parallel$ , which is proportional to  $q^{-1}$ . Naturally, this should occur also in disordered magnetic materials. In the limit  $q \rightarrow 0$  such a contribution obviously determines the behavior of  $G_q^\parallel$ . However, according to Ref. 20 (see also the review in Ref. 21), in the expression for  $G_q^\parallel$  this contribution has a small numerical factor and for finite values of  $q$  the formulas of Eq. (14) may still be valid.

It is shown in Ref. 13 that under the conditions of validity of the formulas in Eq. (14) the correlation function of

longitudinal configuration fluctuations is as follows:

$$\tilde{G}_q^{\parallel} = \tilde{A}^{\parallel} (Q^{\parallel} - M^2) (q^2 + \kappa^2)^{-2}, \quad (15)$$

$$Q^{\parallel} - M^2 = \tilde{B} |\tau|, \quad \tilde{A}^{\parallel} \sim A, \quad (16)$$

where  $Q^{\parallel} = \langle (\mathbf{m}_i^{\parallel})^2 \rangle_c$  is the longitudinal Edwards-Anderson parameter;  $\tilde{B} \propto (T_f/T_c)^2$  when  $T_f \ll T_c$  and  $\tilde{B} \sim 1$  when  $T_f \sim T_c$ .

It follows from Eqs. (15) and (16) that the configuration correlations are absent from ordered magnetic materials, i.e., at  $T_f = 0$ , and also in the case of the P phase at temperatures  $T > T_c$ . Moreover, since in the ergodic ferromagnetism range we have  $Q^{\perp} = \langle (\mathbf{m}_i^{\perp})^2 \rangle_c = 0$  (see Ref. 13), it follows that the corresponding configuration correlation functions vanish:  $\tilde{G}_q^{\perp} = 0$ . Equations (15) and (16) were obtained in Ref. 13 without allowance for the interaction of different types of fluctuations. Therefore, the range of their validity is limited and is probably the same as that of the formulas for the thermodynamic correlations [Eqs. (14) and (9)]. As in Eqs. (14) and (9), we have to assume that  $Q^{\parallel} - M^2 \propto |\tau|^{2\rho}$  and  $\kappa \propto |\tau|^{\nu}$ , where  $\rho$  is a new independent exponent. It is interesting to note that in the range of validity of the molecular field theory we have  $Q^{\parallel} - M^2 \propto \kappa^2$ , where  $\kappa \propto |\tau|^{\nu}$  and  $\nu = 1/2$ . However, this means that the scaling dimensionalities of  $\tilde{G}_q(\kappa)$  and  $G_q(\kappa)$  are equal. If this equality applies also in the critical region near  $E_c$ , then the exponent is  $\rho = \nu$ .

In the F phase we find, as in the P phase, that the F fluctuations in disordered magnetic materials are accompanied also by SS fluctuations. As already mentioned, if  $\xi < 0$ , these fluctuations prevent transition to the state F as a result of cooling. If  $\xi > 0$ , then correlations of the SS order parameter continue to rise also below  $T_c$  and this may result in the formation of a mixed phase or in a phase transition to the SG state at some temperature  $T_g(x) < T_c(x)$ .

### c) Correlations in the spin glass and mixed phases

First of all, we must point out that there have been practically no theoretical investigations of the behavior of spatially inhomogeneous spin correlation functions in the SG state. Therefore, the correlation picture proposed below is based only on very general ideas on the properties of the SG phase and on some estimates which can be drawn employing simple models of this phase. We recall that, according to the current ideas (for a review see Ref. 22), the SS phase is bounded in the phase diagram by the lines of transition from the P phase  $T_f(x)$  and from the F phase  $T_g(x)$ , and that a region where the F and SG properties coexist adjoins directly the SG phase. This mixed phase is separated from the ergodic F state by the phase transition line  $t'_g(x)$ .

Clearly, the correlation radius of the magnetization fluctuations in the SG phase depends on the distance in the phase diagram from the phase exhibiting a spontaneous moment, i.e., by the distance from the phase boundary  $T_g(x)$ . On the other hand, as already pointed out, the SG state is fundamentally of nonequilibrium nature. Therefore, the characteristic scale of these correlations should also depend on the observation time and on the proximity to the boundary  $T_f(x)$  of the transition to the nonequilibrium state.

The correlation radius, like other physical quantities, varies logarithmically slowly with time and it is quite diffi-

cult to observe such variation in neutron experiments. In view of the nonequilibrium nature of the SG state, the observed scattering intensity given by Eq. (8) should include a contribution of the slowly relaxing configuration fluctuations  $\tilde{G}_q$ .

Using the methods of Refs. 15 and 23 we can show that in the case of SG phase when  $q \gg \kappa$ , we have  $\tilde{G}_q \propto q^{-4}$ , whereas in the opposite limiting case the value of  $\tilde{G}_q$  is independent of  $q$ . Therefore,  $\tilde{G}_q$  can be approximated roughly by an expression analogous to Eq. (15):

$$\tilde{G}_q \propto Q (q^2 + \kappa^2)^{-2}. \quad (17)$$

In precisely the same way we find that instead of Eqs. (14)–(16) the mixed (or asperomagnetic A) phase is described by

$$\begin{aligned} \tilde{G}_q^{\perp} &\propto Q^{\perp} (q^2 + \kappa_{\perp}^2)^{-2}, & \tilde{G}_q^{\parallel} &\propto (Q^{\parallel} - M^2) (q^2 + \kappa_{\parallel}^2)^{-2}, \\ \tilde{G}_q^{\perp} &\propto (q^2 + \kappa_{\perp}^2)^{-1}, & Q_q^{\parallel} &\propto (q^2 + \kappa_{\parallel}^2)^{-1}. \end{aligned} \quad (18)$$

It is important to stress that  $\tilde{\kappa}_{\perp}$  and  $\kappa_{\perp}$  may differ to zero only because of the nonergodicity of the state A. Their values, like the values of  $\tilde{\kappa}_{\parallel}$  and  $\kappa_{\parallel}$ , are defined for characteristic observation times.

In the longitudinal correlation functions of  $\mathbf{M}$  the quantities  $Q^{\parallel}$ ,  $\tilde{\kappa}_{\parallel}$ , and  $\kappa_{\parallel}$  relax slowly to their finite equilibrium values and, therefore, we generally have  $\tilde{\kappa}_{\parallel} \neq \tilde{\kappa}_{\perp}$  and  $\kappa_{\parallel} \neq \kappa_{\perp}$ . However, in real experiments the difference between  $\kappa_{\parallel}$  and  $\kappa_{\perp}$  and also between  $\tilde{\kappa}_{\parallel}$  and  $\tilde{\kappa}_{\perp}$  may be small. In fact, the nonequilibrium correction to  $\kappa_{\parallel}$  and  $\tilde{\kappa}_{\parallel}$  and the values of  $\tilde{\kappa}_{\perp}$  and  $\kappa_{\perp}$  depend on the separation from the boundary between the regions of equilibrium and nonequilibrium ferromagnetism  $T'_g$ . On the other hand, the equilibrium parts of  $\tilde{\kappa}_{\parallel}$  and  $\kappa_{\parallel}$  are determined by the proximity to the boundaries of the regions in which the magnetization vanishes. Therefore, if the phase diagram is plotted in such a way that for a given concentration  $x$  the magnetization is weak throughout the investigated range of temperatures, then away from the temperature of the transition to the A state the nonequilibrium correction to the correlation radius may become greater than its equilibrium value. This is precisely the situation which occurs in our experiments discussed below.

We shall conclude this section by noting that the formulas for the configuration correlation functions of systems with a random anisotropic exchange, similar to those given above, had been obtained before in Refs. 24 and 25, and for systems with random magnetic fields in Refs. 26 and 27. The results of application of the formulas of Refs. 26 and 27 to the experimental data are discussed in Ref. 28. Finally, an analysis of the scaling asymptotes of the correlation functions of the configuration fluctuations is given in Ref. 29.

### 3. DESCRIPTION OF EXPERIMENTS

Alloys belonging to the  $\text{Fe}_{80-x}\text{Ni}_x\text{Cr}_{20}$  (at.%) systems with the fcc lattice were investigated by the method of scattering of cold polarized neutrons. The phase diagram of the magnetic state of these alloys of interest to us was plotted in Fig. 1 on the basis of magnetic and neutron-diffraction measurements.<sup>14</sup> The investigated alloys were characterized by nickel concentrations  $x = 21, 24, 26$ , and  $28$ , i.e., very close to the concentration  $x = 25$  corresponding to the tricritical point (the main experimental data will be given for the alloys with  $x = 24$  and  $26$ ). Our samples were rectangular plates of

25 × 8 mm dimensions and of 4-mm thickness along the neutron beam.

Measurements were made using a multidetector system for the study of low-angle scattering of polarized neutrons described in Ref. 30. Detectors (comprising 20 helium counters of the SNM-50 type) were located in a horizontal plane with angular separations between the centers amounting to  $\approx 4 \times 10^{-3}$  rad. In these experiments the system had the following collimation parameters: along the horizontal the angular divergence of the incident  $\theta_h$  and scattered  $\theta'_h$  beams was  $\theta_h = 1.3 \times 10^{-3}$  and  $\theta'_h = 1.7 \times 10^{-3}$ , whereas in the vertical direction the corresponding values were  $\theta_v = 10^{-2}$  and  $\theta'_v = 1.4 \times 10^{-2}$ . The average value of the wavelength over the spectrum was  $\langle \lambda \rangle = 9.9 \text{ \AA}$  ( $\Delta \lambda / \lambda \approx 30\%$ ).

A sample was placed in a vacuum isolated container and immersed in a helium bath in a cryostat. The optimal heat exchange conditions between the sample and the bath were selected by varying the pressure of gaseous helium in the vacuum jacket surrounding the sample. A bifilar heater surrounding the sample made it possible to vary its temperature without creating a magnetic field in the sample. The heat transfer between the sample and the heater was improved by filling the container with gaseous helium. The stabilization system ensured that temperatures of the sample

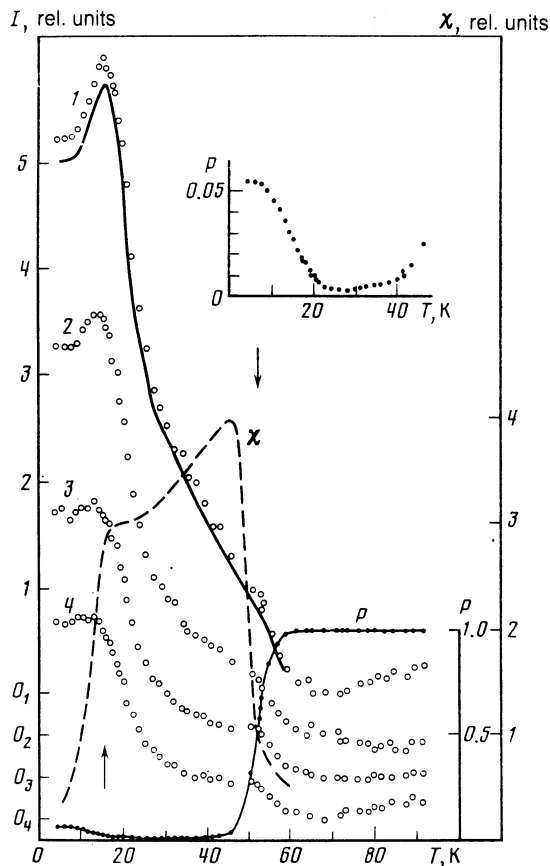


FIG. 2. Temperature dependences of the intensity of the neutron scattering  $I$ , of the neutron polarization  $P$ , and of the magnetic susceptibility  $\chi$  of the alloy with  $x = 26$ : 1)  $q = 4.8 \times 10^{-3} \text{ \AA}^{-1}$ ; 2)  $5.8 \times 10^{-3} \text{ \AA}^{-1}$ ; 3)  $7.4 \times 10^{-3} \text{ \AA}^{-1}$ ; 4)  $8.5 \times 10^{-3} \text{ \AA}^{-1}$ . The upward arrow identifies the position of the scattering maximum  $T_m$  characterized by the minimum transferred momentum, and the downward arrow identifies  $T_c$ . The continuous curve is the dependence  $I(T)$  calculated for  $q = 4.8 \times 10^{-3} \text{ \AA}^{-1}$ . The indices of zeros (on the left) denote here and later the positions of zeros of curves labeled by the relevant numbers.

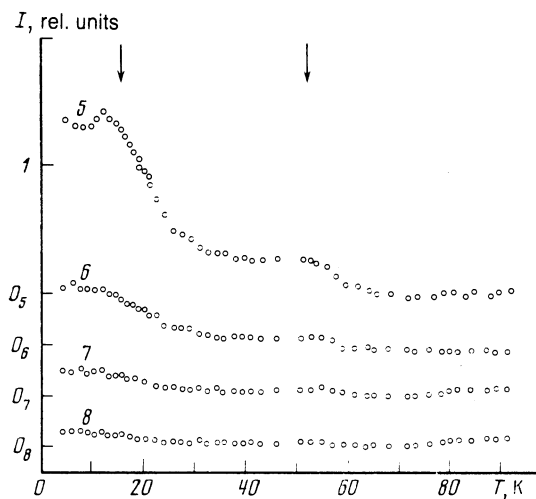


FIG. 3. Dependences  $I(T)$  for the alloy with  $x = 26$  obtained for different transferred momenta: 5)  $q = 1 \times 10^{-2} \text{ \AA}^{-1}$ ; 6)  $1.5 \times 10^{-2} \text{ \AA}^{-1}$ ; 7)  $2.2 \times 10^{-2} \text{ \AA}^{-1}$ ; 8)  $2.7 \times 10^{-2} \text{ \AA}^{-1}$ . The arrows identify the same temperatures as in Fig. 2.

were maintained to within 0.1 K. Protection from uncontrolled external fields was provided by a magnetic screen inside the cryostat. A system of guiding fields ensured that the direction of the polarization vector of neutrons  $\mathbf{P}_0$  was set adiabatically along the axes of a laboratory coordinate system.

The experimental data obtained in one series of measurements on alloys with  $x = 26$  and 24 are plotted in Figs. 2–5. Figures 2 and 3 give the temperature dependences of the scattering intensity  $I(T)$  obtained for different values of  $q = \langle k_0 \rangle \theta_y$  ( $\theta_y$  is the scattering angle in the horizontal plane and  $\langle k_0 \rangle = \langle 2\pi/\lambda \rangle$ ) and of the polarization  $P(T)$  obtained using the central counter and the alloy with  $x = 26$ . The average data-acquisition time at a given temperature was 45 min. The scattered neutron intensity (Figs. 2 and 3) was plotted after subtraction of the background of neutrons scattered by the cryostat and of the background representing the scattering by the sample, measured at  $T = 65\text{--}70 \text{ K}$ .

The scattered neutrons were recorded on both sides of

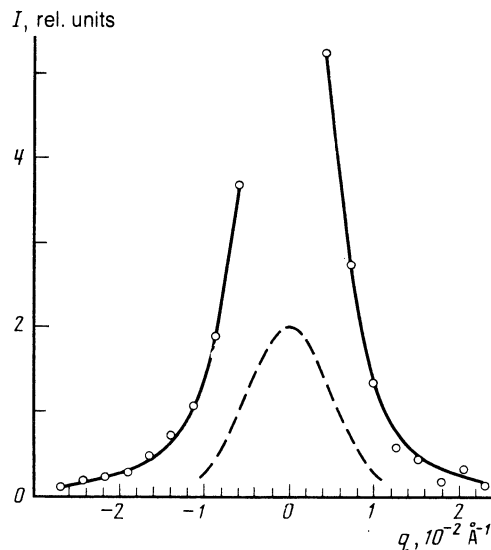


FIG. 4. Dependence  $I(q)$  for the alloy with  $x = 26$  at  $T = 4.5 \text{ K}$ . The continuous curve is calculated, the points are the experimental values, and the dashed curve is the resolution function of the apparatus.

the incident beam. By way of example, we plotted in Fig. 4 the dependence of the intensity of the scattered neutrons on the value of  $q$  for the alloy with  $x = 26$  at  $T = 4.5$  K. The results plotted in Figs. 2 and 3 were obtained without deliberate application of an external magnetic field to the sample, but the presence of a guiding magnetic field, necessary for the polarization analysis and directed in this case along the beam axis ( $z$  axis), meant that the sample experienced a field  $H_z \lesssim 0.3$  Oe.

On the whole, the low-angle scattering pattern was similar to that observed earlier for alloys with an analogous phase diagram of the magnetic states (see, for example, Ref. 4). In particular, the critical scattering in the vicinity of  $T_c$  was weak, as also found earlier.<sup>1,2,4</sup> A clear low-angle scattering peak was observed at  $T \approx 15$  K (Figs. 2 and 3) and its position corresponded to the region of fall of the susceptibility of this alloy recorded at a frequency  $f = 217$  Hz and shown by a dashed curve in Fig. 2. The scattering maximum shifted toward lower temperatures when  $q$  was increased. A similar temperature dependence of the scattered-neutron intensity was observed also for the alloy with the nickel concentration  $x = 28$ , but in this case a reliable resolution of the low-temperature scattering peak was possible only at temperatures below 4.2 K which was impractical in our experiments.

The temperature dependence of the polarization  $P(T)$  of neutrons scattered to the central counter was also determined (Fig. 2). In the high-temperature range this polarization curve was similar to the temperature dependence  $P(T)$  usually observed for ordered magnetic materials undergoing the P-F phase transition. As usual, the polarization in the P phase was equal to the initial polarization  $P_0$  of the beam and it decreased strongly on transition across  $T_c$ . However, the dependence  $P(T)$  observed for our alloys had a number of significant details distinguishing it from the dependences reported earlier for ordered ferromagnets.<sup>31</sup> First of all, we found that in the vicinity of  $T_c$  the polarization fell much less rapidly than in the cases mentioned above, and in the F region it did not vanish for samples of thicknesses of the same order as in Ref. 31. Moreover, as demonstrated by the inset in Fig. 2, a considerable rise of  $P(T)$  began below 30 K. According to the phase diagram of Fig. 1, transition to the SG phase should occur in this region. In the case of the alloys with a higher concentration of Ni ( $x = 28$ ), i.e., with a higher value of  $T_c$  and a lower degree of disorder in the magnetic subsystem, the polarization in the F phase fell to zero and, to within  $10^{-3}$ , remained zero throughout the temperature range right down to  $T = 4.2$  K. According to the phase diagram of Fig. 1, the transition to the SS phase in this alloy should occur at  $T_g \approx 15$  K.

The experimental results obtained for the alloy with the lower Ni content ( $x = 24$ ) are plotted in Fig. 5. In this case, as indicated by the magnetic measurements (Fig. 1), the F phase was absent and a transition occurred from the P to the SS phase at  $T_f = 22$  K. The magnetization and susceptibility measurements were also made (Fig. 6). The temperature dependence of the intensity  $I$  of the scattered neutrons was determined for  $q = 5 \times 10^{-3} \text{ \AA}^{-1}$  (Fig. 5a). The temperature dependence of the polarization  $P(T)$  of neutrons recorded by the central counter ( $q \approx 0$ ) was also recorded (Fig. 5b). All these measurements were made when the tem-

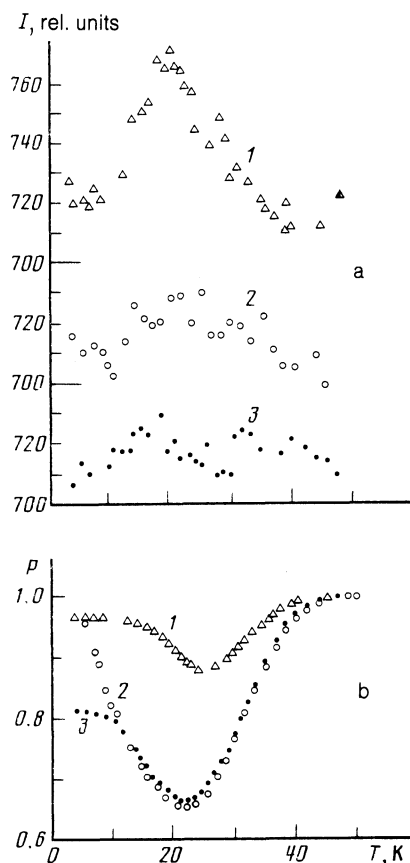


FIG. 5. Temperature dependences of: a) the intensity of the neutron scattering  $I(T)$  by the alloy with  $x = 24$  and  $q \approx 5 \times 10^{-3} \text{ \AA}^{-1}$ ; b) polarization  $P(T)$  of neutrons reaching the central counter, obtained in "zero" magnetic field (1), in a field  $H_x = 62$  Oe after preliminary cooling to 4.2 K in zero field (2), and after cooling to 4.2 K and measurements in a field  $H_x = 62$  Oe (3).

perature of a sample, cooled initially to 4.2 K, was increasing. The results plotted in Fig. 5 and represented by symbols 1 were obtained when both the cooling of the sample and the measurements were carried out in "zero" external field (i.e., in a guiding field of  $H_z \lesssim 0.3$  Oe). The results denoted by 2 were obtained when the sample was cooled in zero field and

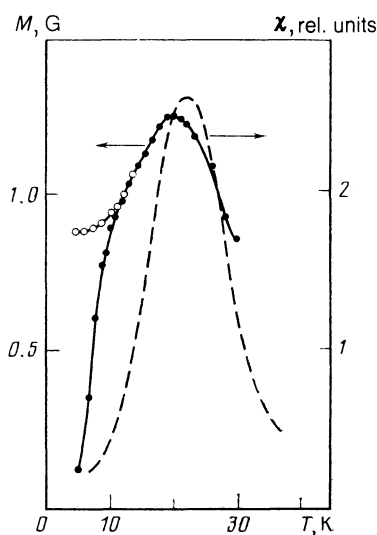


FIG. 6. Temperature dependences of the magnetization  $M$  in a field  $H = 62$  Oe and of the susceptibility  $\chi$  of the alloy with  $x = 24$ : ●) cooling to 4.2 K in zero field; ○) cooling to 4.2 K in a field  $H = 62$  Oe.

the measurements were carried out in a field of  $H_x = 62$  Oe, which was applied at  $T = 4.2$  K (in this case the  $x$  axis was directed vertically, parallel to the long side of the sample). Finally, the results denoted by 3 were obtained when both the preliminary cooling and the measurements during heating were carried out in a field of  $H_x = 6.2$  Oe. It is clear from Fig. 5a that for  $q \approx 5 \times 10^{-3} \text{ \AA}^{-1}$  the scattered-neutron maximum rose by just 5% above the high-temperature background. The temperature of the scattering maximum agreed well with the temperature of the maximum of the susceptibility curve in Fig. 6. A relatively weak field ( $H = 62$  Oe) reduced strongly the maximum of the scattering cross section (compare results denoted by 2 and 3 with those denoted by 1). The scattering decreased strongly on increase in the transferred momentum  $q$ . For example, for  $q > 7.5 \times 10^{-3} \text{ \AA}^{-1}$  the scattering maximum practically disappeared even in zero field.

The polarization decreased as a result of cooling (Fig. 5b) reaching a minimum in the region of the maximum of the low-angle scattering  $I(T)$ . However, it should be pointed out that the minimum of  $P(T)$  did not coincide exactly with the maximum of  $I(T)$ . Further cooling increased the polarization again but it did not reach the values found at higher temperatures. It is clear from this figure that the polarization began to fall at fairly high temperatures ( $\approx 45$  K), i.e., in the far P region of the phase diagram in Fig. 1. This was a very unusual effect, since in the case of disordered ferromagnets the depolarization of neutrons in the P phase has not been observed before. The exception was the direct vicinity of  $T_c$ , where depolarization amounted to a few percent (see Ref. 31), in agreement with the estimates obtained by Maleev and Rubanov.<sup>32</sup> Moreover, an external magnetic field had, at first sight, a very unusual effect on the depolarization. For example, the application of a fairly weak field of  $H = 62$  Oe parallel to  $\mathbf{P}_0$  increased the depolarization almost threefold. However, in the case of ordered magnetic materials an external field usually reduced the depolarization.

It is clear from Fig. 5 that the temperature dependence of the polarization in a field applied at low temperatures depended on the method of cooling, i.e., irreversible changes typical of a strongly degenerate SG phase were observed (see, for example, the reviews in Refs. 6 and 7). A similar irreversibility had been observed before, usually in measurements of the magnetization of a sample under various cooling conditions (see, for example, Ref. 33). The results of such measurements for this alloy were plotted in Fig. 6, where the black dots represent the preliminary cooling in zero field and subsequent measurements of the magnetization in a field  $H = 62$  Oe, whereas the open circles represent cooling and measurements in a field  $H = 62$  Oe. An analysis of the temperature dependences  $P(T)$  and  $M(T)$  in Fig. 6 indicated that the temperatures of appearance of irreversible effects agreed to within better than 1 K.

We shall conclude this section by noting that the low-angle scattering cross section and particularly the polarization were extremely sensitive to small changes in the composition. For example, in the case of the samples with  $x = 28$  and 26 we observed a very strong depolarization of neutrons at low temperatures, whereas in the case of a sample with  $x = 24$  in a field  $H = 0$  the change in the polarization was approximately 13%, whereas for a sample with  $x = 21$  the depolarization did not exceed 0.2%.

We shall not consider here the problems of quantitative interpretation of the results of our depolarization measurements. This will be done in a separate communication where in particular we shall show that such measurements can be used to study the processes of slow relaxation, dependence of such relaxation on the magnetizing field or temperature, etc.

#### 4. ANALYSIS AND INTERPRETATION OF RESULTS

##### a) Selection of the parametrization method

In this section we shall consider the experimental results reported above and use the main concepts on the nature of the spin correlations introduced in Sec. 2. We recall that in addition to the thermodynamic correlations in disordered magnetic materials, the low-temperature phases exhibit also configuration correlations. Moreover, expressions describing these types of correlations were obtained in Ref. 13 for a parametrically defined region of the P and F phases. However, our experimental results were obtained in a wide range of temperatures which could possibly include temperatures where these formulas would be inapplicable. We mentioned already those theoretical problems which can be solved in order to provide a description of the correlation in all the phases of systems with a competing random interaction. At present many of them are the subject of intensive theoretical studies but have not yet been solved. Therefore, it is quite natural to describe the experimental results in terms of the simplest variant of the theory allowing however for the important feature of the possibility of appearance of configuration spin correlations. We shall limit the analysis of our data to the intensity of the low-angle neutron scattering presented in Figs. 2 and 3 in the case of the sample exhibiting the F phase.

First of all, we shall derive an expression which can be used to analyze these data recalling that the spin correlation tensor is anisotropic in the F region. Therefore, the scattering cross section includes contributions of the components of this tensor both longitudinal and perpendicular to the magnetization. In principle, as shown in Refs. 34 and 35, these contributions can be found separately in the experiments. We have drawn attention above to the fact that this would be very interesting to do particularly in connection with the problem of asperomagnetism mentioned above. Moreover, if such a separation is not carried out, then even in the simplest case when there is no asperomagnetism, the cross section is governed by the sum of the contributions of three terms [see Eqs. (7) and (8)]. This complicates greatly an ambiguous interpretation of the experimental data, since this would require additional assumptions about them which we shall discuss below.

Allowing for the finite angular resolution, the expression for the scattering intensity  $I(q)$  used in the analysis of the data is as follows:

$$I(q) = \int dp K(p, \kappa) R(q-p). \quad (19)$$

Here,  $R(q-p)$  is the resolution function of the apparatus approximated by a Gaussian function and represented by the dashed curve in Fig. 4. The integrand  $K(p, \kappa)$  is a sum of two terms:

$$K(p, \kappa) = A_1/(p^2 + \kappa^2)^2 + A_2/(p^2 + \kappa^2) = s_1 + s_2. \quad (20)$$

The first term in the above expression should describe the

contribution of the configuration correlations, in accordance with Eqs. (8), (14), and (15), whereas the second corresponds to the thermodynamic correlations.

We analyzed the experimental data presented in Figs. 2 and 3 using Eqs. (19) and (20) and this was done simultaneously for all the scattering angles by the method of least squares. The results were then used to find three independent parameters  $A_1$ ,  $A_2$ , and  $\kappa$  for each temperature  $T$ . For our sample we plotted in Fig. 4 (continuous curve) the dependence of the intensity on  $q$  calculated from Eqs. (19) and (20) at  $T = 4.5$  K. The temperature dependence of the intensity calculated using the parameters deduced by the least-squares method is represented by the continuous curve in Fig. 2. We can see from this figure that the calculated curve reflects all the features of the behavior of the scattering of neutrons characterized by  $q = 4.8 \times 10^{-3} \text{ \AA}^{-1}$ , although it lies somewhat below the experimental points which is probably due to the error in the subtraction of the background. We shall now consider the temperature dependences of the parameters  $\kappa$ ,  $A_1$ , and  $A_2$ .

### b) Temperature dependence of the correlation radius

It is clear from Fig. 7 that the correlation radius  $R_c = \kappa^{-1}$  rises rapidly as a result of cooling in the P region. Unfortunately, the large error prevents us from drawing any definite conclusions on the nature of the rise and thus checking the theoretical predictions in this range. However, it should be pointed out that—in spite of the practically complete absence of the critical scattering maximum in Figs. 2 and 3—the proposed analysis of the data allows us to identify the phase transition region which coincides with the region of a rapid fall of the polarization curve  $P(T)$  in Fig. 2.

In fact, at  $T = T_c$  the parameter  $\kappa$  should vanish and this naturally cannot be observed in real experiments. The precision of direct determination of the Curie temperature is

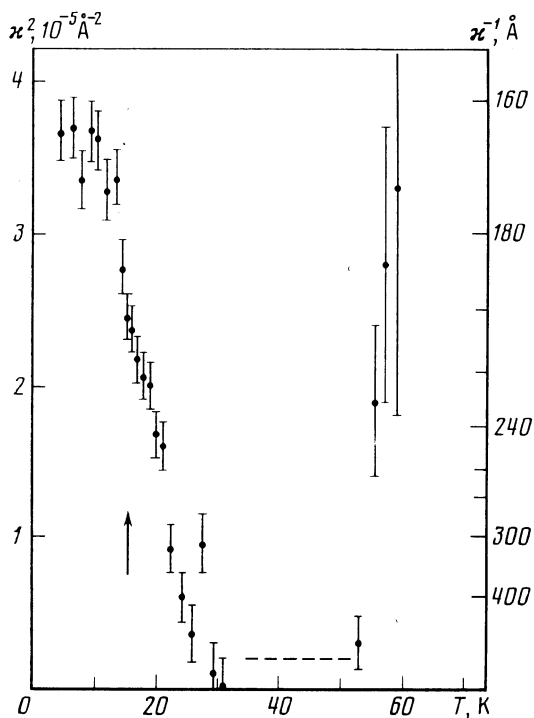


FIG. 7. Temperature dependence of  $\kappa$ . The arrow identifies  $T_m$ .

naturally then limited by the minimum angular resolution of our experiments. We found that the parameter  $\kappa$  became less than the momentum resolution of the apparatus at  $T = 54$  K, which agreed well with the value  $T_c \approx 52$  K found from the magnetic measurements.

Then, in the temperature range from  $T = 54$  K to  $\approx 30$  K the values of this parameter were found to be experimentally indistinguishable from zero. This naturally did not mean that  $\kappa = 0$  was true for the whole region of the F phase. Moreover, we know that the correlation radius  $R_c$  should decrease and its reciprocal should rise away from  $T_c$  also in the F state. However, there are grounds for assuming that throughout the investigated range of temperatures the correlation radius of our system should be anomalously large. In fact, in contrast to ordered magnetic materials, it follows from Eq. (14) that the value of  $\kappa$  contains not only a temperature factor  $\tau$ , but also an additional small factor  $\xi$  representing proximity to the triple point in the phase diagram.

Equation (14) is derived on the assumption that the values of the parameter  $\xi$  are not too small, i.e., that  $\xi \gg \tau$ . Otherwise the correlation radius  $R_c = \kappa^{-1}$  of Eq. (14) should be determined by the separation between a given point in the phase diagram and the triple point. Its value should depend relatively weakly on temperature and it should be governed primarily by the relative concentration  $|x - x_0| x_0^{-1} \ll 1$ , where  $x_0$  is the concentration corresponding to the triple point in the phase diagram of Fig. 1. However, then the parameter  $\kappa(T, x)$  should be small in this range of temperatures and the measure of smallness should be the ratio  $|x - x_0| x_0^{-1}$ .

At lower temperatures the phase boundary of the reentrant SG state should begin to affect the results and the correlation radius should fall again, i.e., the value of  $\kappa$  should rise. In the case of the investigated alloy the experimental resolution was insufficient to observe these effects in the ferromagnetic phase. This was why a relatively rough approximation allowed us to describe the experimental data, obtained throughout the full wide temperature range, by such a simple formula as Eq. (20), containing just three parameters. Otherwise we would have to distinguish between the longitudinal and perpendicular correlations, i.e., we would have had to introduce at least one additional parameter [see Eqs. (14) and (15)].

The nonmonotonic temperature dependence of the angular width of the scattering intensity curve for the F phase had been reported for similar systems in Ref. 4. True, the authors of Ref. 4 ignored completely the possibility of existence of configuration correlations in the F state and they ignored both transverse thermodynamic fluctuations and the contribution of their interaction to the longitudinal correlation function [see Eq. (14) and the discussion in Sec. 2b]. In other words, the results reported in Ref. 4 were obtained by an analysis of the data in accordance with the formula allowing only for the second term in Eq. (20). It should be pointed out that it was mentioned in Ref. 4 that at low temperatures such an analysis did not describe quite satisfactorily the experimental results. We also found that an attempt to analyze our data without allowance for the first term in Eq. (20) provided a much less accurate description of the experiments.

Moreover, we made an unsuccessful attempt to describe the experimental data in a different way. For example, we

replaced Eq. (20) with a dependence of the type  $K(p, \kappa) = A_3(p^2 + \kappa^2)^{-\mu}$ , but this yielded the temperature dependences of the index  $\mu$  and other parameters that were difficult to interpret. In the F region under discussion, defined by the condition  $\kappa = 0$  in Fig. 7, the scattering intensity depended weakly on temperature with the exception of very small values of  $q$  (Fig. 2). Therefore, we checked the validity of Eq. (20) in this range by an analysis of the results using—instead of Eq. (20)—the formula

$$K(p, \kappa) = A_4 q^{-2} + A_5 q^{-\zeta}$$

in which we determined the parameters  $A_4$ ,  $A_5$ , and  $\zeta$ . It was found that we could quite accurately assume that  $\zeta = 4$ , as expected in the case of validity of Eq. (20).

Some qualitative effects predicted in Fig. 7 were similar to those reported in Ref. 4 in the case of the half-width of the angular distribution of the scattering intensity. In particular, an increase in the half-width was reported in Ref. 4 for low temperatures, whereas in our experiments the parameter  $\kappa$  increased. This increase could naturally be explained by a reduction in the correlation radius away from the boundary  $T'_g$  representing the phase transition from the F state to the reentrant SS phase.

It is worth noting that the phase transition temperature deduced from the condition  $\kappa = 0$  was almost twice as large as the value deduced from the magnetic measurements and it amounted to  $T'_g \approx 30$  K. The large difference between the phase transition temperatures obtained by different methods was also reported in Ref. 4. In general, it was not surprising, because the phase transition point corresponded to the appearance of an infinitesimally small magnetization in zero external field throughout the sample, i.e., when  $q = 0$ . Therefore, determination of the transition temperature required extrapolation of the experimental results, such as that carried out in Ref. 3. Moreover, the transition temperatures were frequently given *a priori* values corresponding to certain particular singularities of the temperature dependences of the measured quantities. Traditionally in the neutron experiments it has been assumed that the phase transition temperature can be deduced from the position of the low-angle scattering peak, although it is well known that the position of this peak in the case of ordered magnetic materials depends on the transferred momentum (see Ref. 36 and discussions in Refs. 13 and 34). Similarly the positions of inflections in the temperature dependence of the magnetic susceptibility, identified with the phase transition temperatures (Fig. 2), depend on the intensity of the measuring magnetic field and its frequency. Therefore, the phase diagram of Fig. 1 is to some extent nominal and no particular significance should be attached to the observation that the position of the low-temperature peak of the low-angle scattering in Fig. 2 is outside that region of Fig. 7 where  $\kappa \rightarrow 0$  and  $T'_g \neq T_g$ .

However, several observations (see below) and particularly the excessively large difference between the values of  $T'_g$  and  $T_g$  make it necessary to consider other interpretations of our low-temperature results. It is shown in the preceding section that the transition to the mixed (or asperomagnetic) phase gives rise to a nonequilibrium correction to the reciprocal of the correlation radius and this correction increases as a result of cooling. However, the magnetization does not vanish in the range  $T_g < T < T'_g$ , as would follow

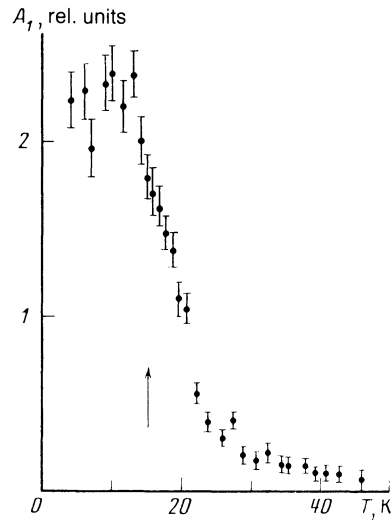


FIG. 8. Temperature dependence of  $A_1$ . The arrow identifies  $T_m$ .

from direct measurements.<sup>14</sup> The interpretation of  $T'_g = 30$  K as the phase transition temperature to a nonequilibrium ferromagnetic state is supported also by the temperature dependences of the parameters  $A_1$  and  $A_2$  in Eq. (20).

### c) Temperature dependences of the amplitudes $A_1$ and $A_2$

It is clear from Figs. 8 and 9 that in the F region, defined by the condition  $\kappa = 0$ , the parameter  $A_2$  is independent (within the limits of the experimental error) of temperature, in agreement with Eqs. (20) and (14). It changes somewhat in the direct vicinity of  $T_c$ , which is not in conflict with Eqs. (9) and (14). The numerator of the first term in Eq. (20), which is  $A_1$ , also differs from zero for the F phase. In the temperature range  $T'_g \lesssim T \lesssim T_c$  it is small and depends weakly on  $T$ . At low temperatures  $T \lesssim T'_g$  both  $A_1$  and  $A_2$  begin to rise and the rise of  $A_1$  is much faster than that of  $A_2$ .

The temperature dependence of  $A_1(T)$  is readily explained if we assume that an asperomagnetic transition does indeed occur at  $T = T'_g$ . In fact, as pointed out already, well inside the F phase region the correlation radius and, conse-

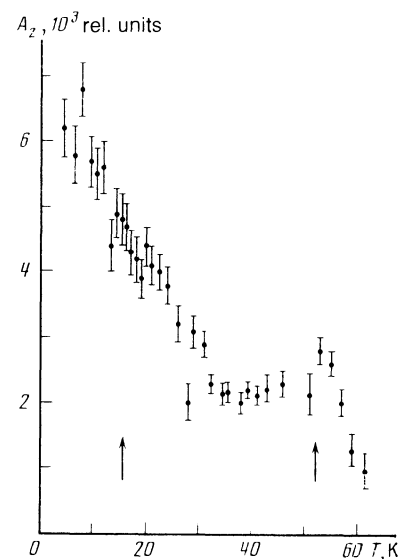


FIG. 9. Temperature dependence of  $A_2$ . The arrow identifies  $T_m$ .

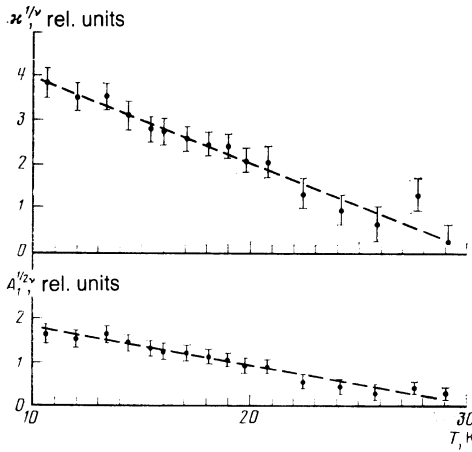


FIG. 10. Temperature dependences of  $\chi^{1/\nu}$  and  $A_1^{1/2\nu}$  for  $\nu = 0.65$ .

quently, the magnetization  $\mathbf{M}$  as well as the Edwards-Anderson parameter  $Q^{\parallel}$  should depend weakly on temperature for  $|x - x_0| x_0^{-1} \ll 1$ . For the same reason that the parameter  $\kappa$  is small in the range  $T'_g < T < T_g$ , the quantities  $\mathbf{M}$  and  $Q^{\parallel}$  should be small, i.e., the parameter  $A_1$  should also be small. Below the transition temperature we can expect nonequilibrium and almost isotropic (because of the smallness of  $\mathbf{M}$ ) spin fluctuations, so that  $Q^{\parallel} \approx Q^{\perp}$  [see Eq. (17)]. Further cooling increases the degree of nonequilibrium of the system so that the quantities  $Q^{\parallel}$  and  $Q^{\perp}$  increase and the parameter  $A_1$  rises with them.

#### d) Scaling parametrization of the temperature dependences $\kappa(T)$ and $A(T)$

If we assume that below the transition temperature  $T'_g$  the correlation radius depends on the relative temperature  $\tau = |T - T'_g|/T'_g$  in accordance with a power law, we can analyze the data of Fig. 7 in accordance with the formula

$$\kappa = \kappa_0 \tau^{-\nu_1}. \quad (21)$$

This gives the following values of the fitting parameters:

$$\nu_1 = 0.65 \pm 0.05, T'_g = (31 \pm 1) \text{ K}, \kappa_0 = (8 \pm 2) \cdot 10^{-3} \text{ \AA}^{-1}.$$

The degree to which the power law (21) for the reciprocal correlation radius  $\kappa$  is obeyed can be judged on the basis of the data plotted in the upper part of Fig. 10. In the lower half of this figure the data on  $A_1$  are expressed in a form demonstrating the power-law dependence:

$$A_1 = A_0 \tau^{2\nu_2}. \quad (22)$$

Within the limits of the experimental error it is found that not only the transition temperatures  $T'_g = 31 \text{ K}$  deduced from Eqs. (21) and (22) agree, but this is also true of the exponents  $\nu_1$  and  $\nu_2$ , i.e., we have  $\nu_1 \approx \nu_2 \approx \nu$ . It is interesting to note that this value agrees well with the exponent of the correlation radius  $\nu \approx 2/3$  for the F-P transition in ordinary ordered magnetic materials. Moreover, the equality  $\nu_1 \approx \nu_2$  ensures an approximately the same scaling temperature dependence of the configuration and thermodynamic correlations. The ratio of their contributions in the investigated range of temperatures and momenta can be judged on the basis of Fig. 11. Bearing in mind these circumstances we can say, with the degree of precision characteristic of our study, that the following relationship is obeyed:

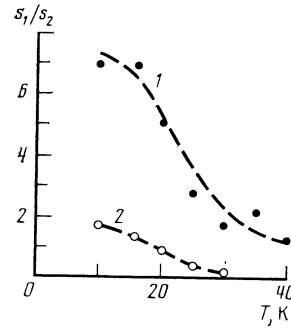


FIG. 11. Temperature dependences of  $s_1/s_2$  for different transferred momenta: 1)  $q = 5.8 \times 10^{-3} \text{ \AA}^{-1}$ ; 2)  $q = 1.6 \times 10^{-2} \text{ \AA}^{-1}$ .

$$s(q, T) \propto G^{\parallel}(q, T) + \tilde{G}^{\parallel}(q, T) \propto \tau^{-\gamma} g'(q/\kappa), \quad (23)$$

where  $\gamma \approx 2\nu \approx 4/3$  is the susceptibility power exponent. It should be noted that the value of the exponent  $\gamma$  obtained in this way is close to that deduced from a scaling analysis of the magnetic measurements in Ref. 3 applied to similar systems undergoing the same phase transition. This is not trivial, because the magnetic susceptibility (as mentioned above) is related directly only to the thermodynamic spin correlations and not to the configuration correlations. It is also clear from Fig. 11 that the role of the configuration correlations rises as a result of cooling. Moreover, their relative contribution is greater in the case of small transferred momenta.

Finally, we can make another very important observation on the basis of Figs. 7–10. It is that the critical behavior of the investigated transition is observed in an unusually wide temperature range  $T = 15\text{--}30 \text{ K}$ . This is due to the anomalously small value of the scaling parameter  $\kappa_0$ , which is explained by the proximity to the triple point of the phase diagram, i.e., by the factor which is responsible for the large value of the correlation radius throughout the F range.

The authors are grateful to S. V. Maleev and G. M. Drabkin for valuable discussions and their interest, to G. A. Takže, A. M. Kostyshin, and I. I. Sych for supplying the samples and the results of magnetic measurements, and to G. P. Gordeev, R. Z. Yagud, V. A. Ul'yarov, V. N. Slyusar', V. P. Grigor'ev, T. A. Zavarukhin, V. I. Volkov, É. B. Rodzevich, I. N. Ivanov, V. V. Deriglazov, B. M. Kholkin, and E. M. Pavlenko for their help in this investigation.

<sup>1</sup>H. Maletta and W. Felsch, Z. Phys. B **37**, 55 (1980).

<sup>2</sup>S. M. Shapiro, C. R. Fincher Jr., A. C. Palumbo, and R. D. Parks, Phys. Rev. B **24**, 6661 (1981).

<sup>3</sup>Y. Yeshurun, M. B. Salamon, K. V. Rao, and H. S. Chen, Phys. Rev. B **24**, 1536 (1981).

<sup>4</sup>G. Aeppli, S. M. Shapiro, R. J. Birgeneau, and H. S. Chen, Phys. Rev. B **28**, 5160 (1983).

<sup>5</sup>D. Sherrington and S. Kirkpatrick, Phys. Rev. Lett. **35**, 1792 (1975).

<sup>6</sup>C. Y. Huang, J. Magn. Mater. **51**, 1 (1985).

<sup>7</sup>S. L. Ginzburg, in: Physics of the Condensed State (Proc. Sixth School at Leningrad Institute of Nuclear Physics) [in Russian], Leningrad (1982), p. 43.

<sup>8</sup>A. P. Young, J. Phys. C **14**, L1085 (1981).

<sup>9</sup>R. Rammal, G. Toulouse, and M. A. Virasoro, Rev. Mod. Phys. **58**, 765 (1986).

- <sup>10</sup>S. L. Ginzburg, Zh. Eksp. Teor. Fiz. **91**, 2171 (1986) [Sov. Phys. JETP **64**, 1291 (1986)].
- <sup>11</sup>L. Lundgren, P. Svedlindh, P. Nordblad, and O. Beckman, Phys. Rev. Lett. **51**, 911 (1983).
- <sup>12</sup>M. Gabay and G. Toulouse, Phys. Rev. Lett. **47**, 201 (1981).
- <sup>13</sup>V. V. Runov, S. L. Ginzburg, B. P. Toperverg *et al.*, Preprint No. 1041 [in Russian], Institute of Nuclear Physics, Leningrad (1985).
- <sup>14</sup>G. A. Takzei, I. I. Sych, A. M. Kostyshin, and V. A. Rafalovskii, Metallofizika (Kiev) **5**, 113 (1983).
- <sup>15</sup>S. L. Ginzburg, Zh. Eksp. Teor. Fiz. **90**, 754 (1986) [Sov. Phys. JETP **63**, 439 (1986)].
- <sup>16</sup>W. Kinzel and K. H. Fischer, Solid State Commun. **23**, 687 (1977).
- <sup>17</sup>G. Aeppli, S. M. Shapiro, R. J. Birgeneau, and H. S. Chen, Phys. Rev. B **29**, 2589 (1984).
- <sup>18</sup>B. P. Toperverg, in: Physics of the Condensed State (Proc. Fourteenth School at the Leningrad Institute of Nuclear Physics) [in Russian], Leningrad (1982), p. 95; Preprint No. 966 [in Russian], Institute of Nuclear Physics, Leningrad (1984).
- <sup>19</sup>A. I. Okorokov, V. V. Runov, B. P. Toperverg, A. D. Tret'yakov, E. I. Mal'tsev, I. M. Puzei, and V. E. Mikhailova, Pis'ma Zh. Eksp. Teor. Fiz. **43**, 390 (1986) [JETP Lett. **43**, 503 (1986)].
- <sup>20</sup>V. G. Vaks, A. I. Larkin, and S. A. Pikin, Zh. Eksp. Teor. Fiz. **53**, 281 (1967) [Sov. Phys. JETP **26**, 188 (1968)].
- <sup>21</sup>S. V. Maleev, Preprint No. 1038 [in Russian], Institute of Nuclear Physics, Leningrad (1985).
- <sup>22</sup>K. H. Fischer, Phys. Status Solidi B **116**, 357 (1983).
- <sup>23</sup>S. L. Ginzburg, Zh. Eksp. Teor. Fiz. **84**, 388 (1983) [Sov. Phys. JETP **57**, 225 (1983)].
- <sup>24</sup>S. L. Ginzburg, Zh. Eksp. Teor. Fiz. **81**, 1389 (1981) [Sov. Phys. JETP **54**, 737 (1981)].
- <sup>25</sup>S. L. Ginzburg, Zh. Eksp. Teor. Fiz. **80**, 244 (1981) [Sov. Phys. JETP **53**, 124 (1981)].
- <sup>26</sup>H. S. Kogon and D. J. Wallace, J. Phys. A **14**, L527 (1981).
- <sup>27</sup>D. Mukamel and E. Pytte, Phys. Rev. B **25**, 4779 (1982).
- <sup>28</sup>R. J. Birgeneau, R. A. Cowley, G. Shirane, and H. Yoshizawa, J. Stat. Phys. **34**, 817 (1984).
- <sup>29</sup>R. A. Pelcovits and A. Aharony, Phys. Rev. B **31**, 350 (1985).
- <sup>30</sup>V. E. Mikhailova, L. A. Aksel'rod, G. P. Gordeev *et al.*, Preprint No. 696 [in Russian], Institute of Nuclear Physics, Leningrad (1981).
- <sup>31</sup>A. I. Okorokov, V. V. Runov, A. G. Gukasov, and G. M. Drabkin, Izv. Akad. Nauk SSSR Ser. Fiz. **42**, 1770 (1978).
- <sup>32</sup>S. V. Maleev and V. A. Ruban, Zh. Eksp. Teor. Fiz. **62**, 416 (1972) [Sov. Phys. JETP **35**, 222 (1972)].
- <sup>33</sup>S. Nagata, P. H. Keesom, and H. R. Harrison, Phys. Rev. B **19**, 1633 (1979).
- <sup>34</sup>S. V. Maleev (Maleyev) and B. P. Toperverg, Solid State Commun. **45**, 1017 (1983).
- <sup>35</sup>B. P. Toperverg, Preprint No. 966 [in Russian], Institute of Nuclear Physics, Leningrad (1984).
- <sup>36</sup>R. Anders and K. Stierstadt, Solid State Commun. **39**, 185 (1981).

Translated by A. Tybulewicz